

Distribution, Elimination, and Toxicity of Silver Nanoparticles and Silver Ions in Rats after 28-Day Oral Exposure

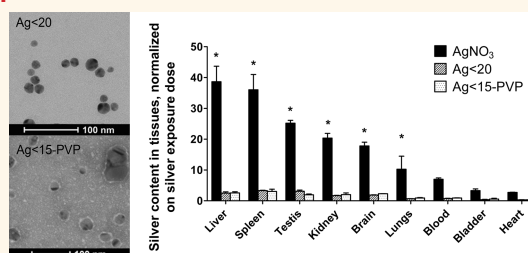
Meike van der Zande,^{†,*} Rob J. Vandebriel,[‡] Elke Van Doren,[§] Evelien Kramer,[†] Zahira Herrera Rivera,[†] Cecilia S. Serrano-Rojero,[†] Eric R. Gremmer,[‡] Jan Mast,[§] Ruud J. B. Peters,[†] Peter C. H. Hollman,[†] Peter J. M. Hendriksen,[†] Hans J. P. Marvin,[†] Ad A. C. M. Peijnenburg,[†] and Hans Bouwmeester[†]

[†]RIKILT—Wageningen University & Research Centre, 6700 AE Wageningen, The Netherlands, [‡]National Institute for Public Health and the Environment, 3721 MA Bilthoven, The Netherlands, and [§]CODA-CERVA—Veterinary and Agrochemical Research Centre, 1180 Uccle, Belgium

The bactericidal effect of silver nanoparticles (AgNPs) has resulted in their worldwide use in several consumer products such as fabrics, deodorants, filters, toothpaste, washing machines, toys and humidifiers.^{1–4} Also in the food and feed industry, the use of AgNPs is growing, for instance in packaging materials, nursing bottles and kitchen utensils. The exact mechanism underlying the antibacterial activity of AgNPs is still unresolved, but literature suggests that these particles interact with the membranes of bacteria.⁴ These efficient interactions increase with decreasing particle size and have been associated with the relatively large surface area to volume ratio of nanoparticles in comparison to their bulk counterparts.⁵ However, these intrinsic properties of AgNPs also render them potentially harmful to humans. It is generally agreed that upon ingestion nanoparticles can be absorbed and that absorption increases with decreasing particle size.⁶

Exposure to AgNPs in animal studies is usually performed by administration of an AgNP suspension. However, AgNPs in suspension have been described to release silver ions,^{7–9} and there is a broad agreement that these silver ions strongly contribute to the biological activity of AgNPs. Several studies have reported strong influences of size, coating, concentration, temperature, ionic strength, or time on the dissolution behavior of silver nanoparticles.^{9–11} Nevertheless, in many *in vivo* and *in vitro* exposure studies the need for characterization of the soluble silver fraction in AgNP suspensions is still ignored. Crucial information might therefore be missed, possibly resulting in a (partially) wrong interpretation

ABSTRACT



We report the results of a 28-day oral exposure study in rats, exposed to <20 nm noncoated, or <15 nm PVP-coated silver nanoparticles ([Ag] = 90 mg/kg body weight (bw)), or AgNO₃ ([Ag] = 9 mg/kg bw), or carrier solution only. Dissection was performed at day 29, and after a wash-out period of 1 or 8 weeks. Silver was present in all examined organs with the highest levels in the liver and spleen for all silver treatments. Silver concentrations in the organs were highly correlated to the amount of Ag⁺ in the silver nanoparticle suspension, indicating that mainly Ag⁺, and to a much lesser extent silver nanoparticles, passed the intestines in the silver nanoparticle exposed rats. In all groups silver was cleared from most organs after 8 weeks postdosing, but remarkably not from the brain and testis. Using single particle inductively coupled plasma mass spectrometry, silver nanoparticles were detected in silver nanoparticle exposed rats, but, remarkably also in AgNO₃ exposed rats, hereby demonstrating the formation of nanoparticles from Ag⁺ *in vivo* that are probably composed of silver salts. Biochemical markers and antibody levels in blood, lymphocyte proliferation and cytokine release, and NK-cell activity did not reveal hepatotoxicity or immunotoxicity of the silver exposure. In conclusion, oral exposure to silver nanoparticles appears to be very similar to exposure to silver salts. However, the consequences of *in vivo* formation of silver nanoparticles, and of the long retention of silver in brain and testis should be considered in a risk assessment of silver nanoparticles.

KEYWORDS: silver nanoparticles · oral exposure · *in vivo* · distribution · elimination · toxicity

of the data. Therefore, the AgNP dissolution behavior should be characterized extensively when using AgNP suspensions for oral exposure, and AgNP exposure studies should also include a treatment with silver ions only. Only then, the effect of the AgNPs *per se* can be studied. At present, distribution and (sub)chronic toxicity data on oral exposure of AgNPs is still scarce. Tissue distribution profiles were described in 28-day and

* Address correspondence to meike.vanderzande@wur.nl.

Received for review June 15, 2012 and accepted August 2, 2012.

Published online August 02, 2012
10.1021/nn302649p

© 2012 American Chemical Society

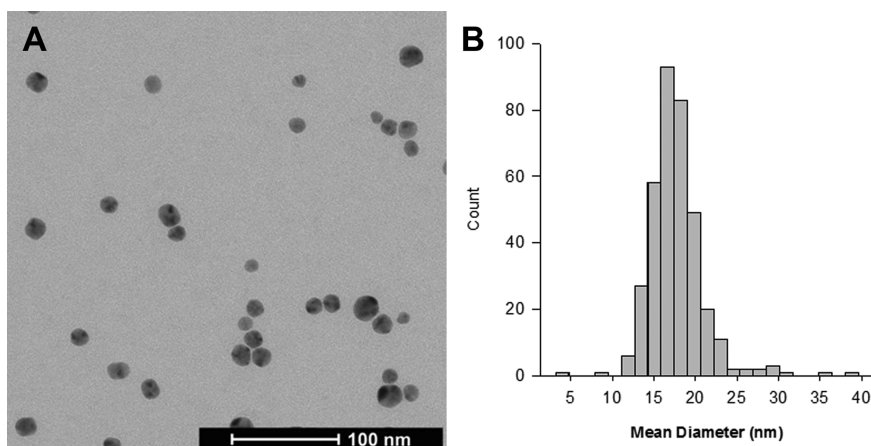


Figure 1. TEM analysis of Ag < 20 silver nanoparticles (NM-300K; ID no. 0454). (A) A representative micrograph showing AgNPs and (B) histogram representing the number-based distribution of the mean core diameter of the AgNPs. Scale bar: 100 nm.

90-day oral exposure studies.^{4,8,12} However, in all these studies only one type of AgNP was used, precluding evaluation of the influence of the coating or size of the particles on the distribution profile. Furthermore, none of the studies used particles that were approved for testing in the Organization for Economic Cooperation and Development (OECD) testing program, nor did they examine the elimination of silver from the organs in time. Next to biodistribution, toxicity parameters have been evaluated in two oral exposure studies,^{4,12} but both studies lacked a silver ion group for comparison, leaving a crucial knowledge gap on the toxicity evaluation of AgNPs in comparison to silver ions.

Therefore, the aim of the present study was to examine the toxicokinetics and tissue distribution of two types of AgNPs and of silver ions in rats, following a 28-day daily repeated oral exposure, with a wash-out period of up to two months. Relatively small AgNPs were selected, since distribution and accumulation of smaller particles is expected to be higher and more widespread than those of larger particles.^{13,14} We selected AgNPs (Ag < 20) that are approved for testing in the OECD program, and have an average size < 20 nm. In addition, coated AgNPs (Ag < 15-PVP), having an average size < 15 nm and a 75 wt % polyvinylpyrrolidone (PVP) coating, according to the manufacturer, were selected. The physicochemical characteristics and the dissolution behavior of the AgNPs in suspension were characterized by transmission electron microscopy (TEM), dynamic light scattering (DLS), ultraviolet–visible (UV–vis) spectroscopy and atomic absorption spectroscopy (AAS). To assess tissue distribution *in vivo*, total silver contents were determined with AAS in a broad range of organs, blood, and intestinal contents. Furthermore, single particle inductive coupled plasma mass spectroscopy (SP-ICP–MS) was applied to detect silver containing nanoparticles in a selection of these organs and in intestinal contents.

The elimination of accumulated silver in the various organs and blood was investigated by AAS and SP-ICP–MS 1 and 8 weeks after the last exposure. Hepatotoxicity was monitored by analysis of alanine aminotransferase (ALT) and aspartate aminotransferase (AST) levels in plasma and immunotoxicity by testing the proliferation of T- and B-cells isolated from spleen and mesenteric lymph nodes (MLN) in response to lipopolysaccharides (LPS) or Concanavalin A (ConA). Also, cytokine levels in culture media from these proliferating T- and B-cells, and the activity of natural killer (NK)-cells isolated from the spleen were measured. Finally, antibody levels in blood were evaluated.

RESULTS AND DISCUSSION

Characterization of AgNPs Suspensions. The size distributions of the two AgNP types were determined by TEM and DLS. TEM indicated an average particle core size of 17.7 ± 3.3 nm for the Ag < 20 particles, with a monomodal distribution of the particles (Figure 1). These results corroborate the publicly available characterization data provided by the manufacturer.¹⁵ The Ag < 15-PVP particles had a mean particle core size of 12.1 ± 8.0 nm. However, unlike the Ag < 20 particles, their size distribution was bimodal (Figure 2). Particles were distributed in two size ranges of which ~75% of the total amount of the particles had a core size < 15 nm, with a maximum peak at 10 nm. The remaining particles (~25%) had core sizes ranging from 15 up to 62 nm, with a peak at ~22 nm. According to the characterization data provided by the manufacturer, the silver core of the particles is < 15 nm, which was confirmed for ~75% of the particles. The PVP coating of the Ag < 15-PVP particles was clearly visible as a white corona after negative staining with uranyl acetate (Figure 2C) and the thickness of the coating was approximately 4–6 nm.

DLS results indicated three peaks within the size range of the hydrodynamic particle size for the Ag < 20 particles.

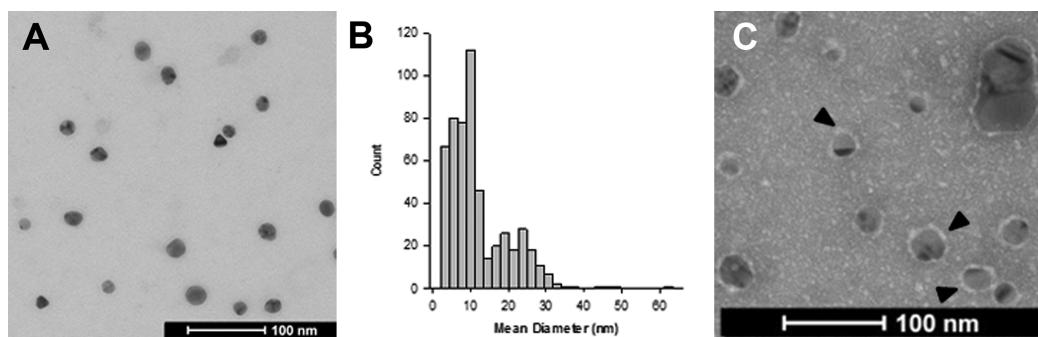


Figure 2. TEM analysis of PVP coated nanoparticles (Ag < 15-PVP). (A) Representative micrograph showing AgNPs, (B) histogram representing the number-based distribution of the mean core diameter of the PVP coated AgNPs, and (C) representative micrograph of negatively stained PVP coated AgNPs, showing the PVP coating as an electron-lucent corona surrounding the AgNPs (arrowheads). Scale bars: 100 nm.

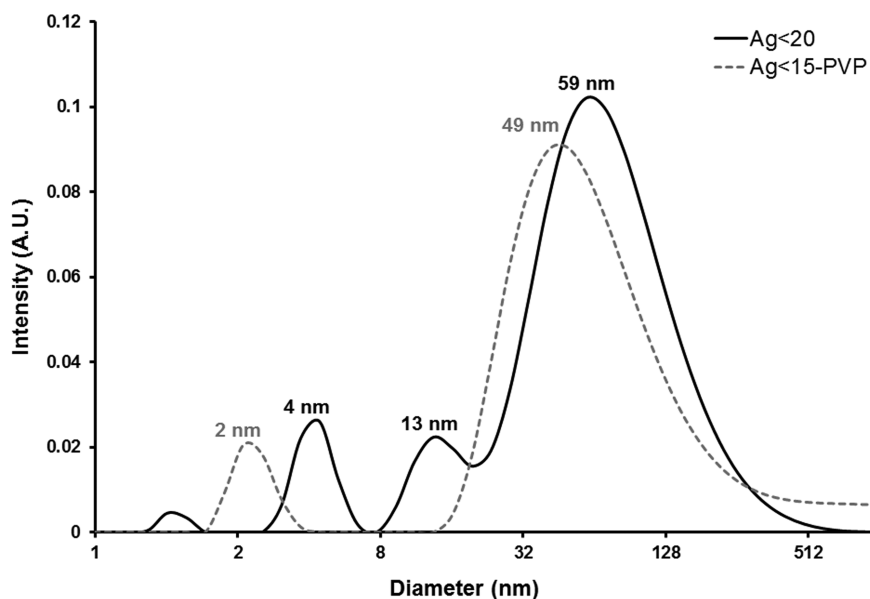


Figure 3. Hydrodynamic diameters of Ag < 20 and Ag < 15-PVP particles, measured with DLS.

The largest peak, with a maximum at 59 nm, consisted of $\sim 80\%$ of the total volume. The other two peaks, with maxima at 4 and 13 nm, consisted each of approximately 10% of the total volume (Figure 3). The particle size distribution of the Ag < 15-PVP particles consisted of two peaks. The largest peak, comprising $\sim 90\%$ of the total volume, had a maximum at 49 nm, while the maximum of the smaller peak, consisting of $\sim 10\%$ of the total volume, was located at 2 nm (Figure 3). The hydrodynamic size distribution curves of both the Ag < 20 and Ag < 15-PVP particles remained stable up to five months (data not shown).

In comparison to the TEM data, DLS measurements indicated a larger size for both particles. It is well-known that DLS measurements are biased toward a larger size, because DLS measures the hydrodynamic size of particles, which includes both the core and the coating, while EM measures only the electron dense core of dried nanoparticles.^{16,17} Particles used in this study are surrounded by the PVP coating (Ag < 15-PVP) or by the stabilizing agents (Ag < 20; polyoxyethylene

glycerol trioleate and polyoxyethylene (20) sorbitan monolaurate (Tween 20)), adding to the hydrodynamic diameter. Furthermore, as an artifact of the DLS methodology, larger particles will overshadow smaller particles. As a result, only a small amount of slightly larger particles present in the suspension, will already greatly influence the maximum particle size of a peak. Also, the two smaller peaks at 4 and 13 nm in the DLS data of the Ag < 20 particle suspension and the peak at 2 nm for the Ag < 15-PVP particles suspension do not correspond to the TEM data. It should be considered that the smaller peak at 4 nm for the Ag < 20 particles, and the smaller peak at 2 nm for the Ag < 15-PVP particles were caused by noise. The peak at 13 nm for the Ag < 20 particles might represent micelle structures of the stabilizers instead of the AgNPs.

For the Ag < 20 suspensions to be given to the rats, we calculated a total silver concentration of 27 mg/mL, based on information given by the supplier. This corresponded nicely with the measured total silver concentration of 25.9 ± 1.9 mg/mL. In contrast, the

TABLE 1. Total Silver Content (Mean \pm SD, $n = 2$) in AgNP Suspension Dilution Series, Ultrafiltered Immediately after Dilution

[Ag] in $\mu\text{g/mL}$	Ag < 20 before ultrafiltration [Ag] in $\mu\text{g/mL}$	Ag < 20 after ultrafiltration [Ag] in $\mu\text{g/mL}$	% of Ag^+
100	111.1 \pm 0.395	6.20	5.5
50	48.0 \pm 4.523	3.10 \pm 0.186	6.5 \pm 1.0
25	18.6 \pm 5.304	1.45 \pm 0.053	8.1 \pm 2.0
10	7.7 \pm 0.871	0.50 \pm 0.022	6.5 \pm 0.4
5	3.4 \pm 0.206	0.24 \pm 0.029	7.0 \pm 0.4

[Ag] in $\mu\text{g/mL}$	Ag < 15-PVP before ultrafiltration [Ag] in $\mu\text{g/mL}$	Ag < 15-PVP after ultrafiltration [Ag] in $\mu\text{g/mL}$	% of Ag^+
100	98.8 \pm 0.001	6.50 \pm 0.184	6.6 \pm 0.2
50	49.4 \pm 0.001	3.32 \pm 0.092	6.7 \pm 0.2
25	23.4 \pm 1.838	1.82 \pm 0.001	7.8 \pm 0.6
10	8.8 \pm 0.001	0.63 \pm 0.028	7.1 \pm 0.3
5	4.7 \pm 0.092	0.29 \pm 0.009	6.2 \pm 0.3

measured total silver content in the Ag < 15-PVP suspension was determined to be 12.5 ± 0.8 mg/mL, 2-fold lower than the calculated total silver concentration of 27 mg/mL. In this calculation, the 75 wt % PVP coating of the particles was already taken into account. It remains unclear what causes this difference.

AgNP dissolution behavior was studied by means of ultrafiltration over a 3 kDa membrane. DLS and UV–vis spectroscopy analysis of the filtrates assured that no particles crossed the membrane (data not shown) and filtration of a dilution series of AgNO_3 indicated an average recovery of silver of $92 \pm 5\%$ after filtration, independent of the concentration. Loss of ions due to binding to the filter was therefore regarded negligible. Initially, AgNP dispersions at a concentration of 27 mg silver/mL were used for oral exposure, but clogging and/or rupture of the filter in the ultrafiltration procedure made it impossible to determine the soluble silver content at such a high concentration. Hence, dilution series of the two AgNP suspensions were analyzed and the impact of dilution on the silver ion dissolution was assessed. These results were used to evaluate whether the ionic content measured in these series could be extrapolated to the ionic content in the suspensions that were administered to the rats. Both AgNP suspensions behaved similarly and appeared to be stable at all concentrations with an average silver ion content of $\sim 7\%$ (Table 1). Therefore, it was regarded fair to assume that the soluble silver content in both suspensions of 27 mg/mL, administered to the rats, would also amount to 7%, at least immediately after preparation. The absence of a concentration-dependent effect on the dissolution behavior of AgNPs has been described earlier,^{10,11} as well as the effect of time,^{9–11} but to our knowledge, so far no study compared polyoxyethylene glycerol trioleate/Tween 20 stabilized particles and PVP-coated particles.

TABLE 2. Total Silver Content (Mean \pm SD, $n = 2$) in a AgNP Suspension, in Which Ultrafiltration Was Performed after Various Time Periods

time	Ag < 20 before ultrafiltration [Ag] in $\mu\text{g/mL}$	Ag < 20 after ultrafiltration [Ag] in $\mu\text{g/mL}$	% of Ag^+
	22.0 \pm 0.8		
0 h		1.22 \pm 0.002	5.8 \pm 0.4
1 h		1.32 \pm 0.020	6.2 \pm 0.6
3 h		1.32 \pm 0.064	6.3 \pm 0.2
6 h		1.40 \pm 0.001	6.6 \pm 0.5
24 h		1.44 \pm 0.006	6.8 \pm 0.6
48 h		1.31 \pm 0.075	6.2 \pm 0.8
7d		1.35 \pm 0.051	6.4 \pm 0.8

time	Ag < 15-PVP before ultrafiltration [Ag] in $\mu\text{g/mL}$	Ag < 15-PVP after ultrafiltration [Ag] in $\mu\text{g/mL}$	% of Ag^+
	8.0 \pm 0.1		
0 h		1.09 \pm 0.066	13.6 \pm 0.6
1 h		1.81 \pm 0.097	22.6 \pm 0.9
3 h		2.29 \pm 0.199	28.7 \pm 2.1
6 h		2.95 \pm 0.284	36.9 \pm 4.1
24 h		2.84 \pm 0.188	35.5 \pm 2.9
48 h		3.10 \pm 0.139	38.8 \pm 2.3
7d		3.62 \pm 0.162	45.3 \pm 2.7

During the study, AgNP suspensions were freshly prepared three times a week just before exposure, so suspensions were used up to a maximum of 2 days after preparation. Therefore, the influence of time on the dissolution behavior of the particles was also studied (Table 2). The Ag < 20 suspension remained stable with an average soluble silver content of $6\% \pm 0.3$ during 7 days. In contrast, ion dissolution of the Ag < 15-PVP particles appeared to be highly time dependent, as the ion content increased up to 45% after 7 days. This makes it impossible to accurately predict the soluble silver content to which the rats of the Ag < 15-PVP groups were exposed, but, compared to the Ag < 20 groups, the soluble silver content could possibly be up to four times higher. Comparing the percentage of Ag^+ of the Ag < 15-PVP at 0 h of Table 2 with the percentage of Ag^+ of the Ag < 15-PVP in the last column of Table 1, one should expect similar results. However, the dissolution of Ag^+ is rather fast and these differences might be caused by small differences between the experiments. It could be speculated that the high release of silver ions from the Ag < 15-PVP particles would lead to a decrease in size of the particles, but DLS data showed that there were no changes in size of the particles in time. However, the weight and diameter of a spherical particle are related by the third power, so a release of 45% of Ag^+ would only reduce the diameter slightly, and DLS is not suitable to measure such minute changes, as was described in this paper earlier.

Even though there are, to our knowledge, no published studies that compared polyoxyethylene

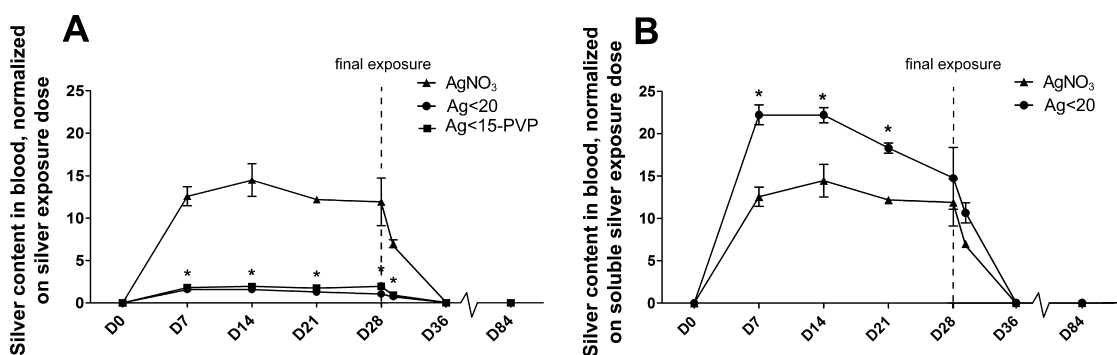


Figure 4. Silver content in blood (mean \pm SEM, $n = 5$) during 84 days. (A) The blood silver content normalized on the daily silver exposure dose is presented as a ratio between the measured silver concentration in blood (μg silver/kg blood) and the daily silver (Ag ions and AgNPs) exposure dose (mg silver/kg body weight). (B) The blood silver content normalized on the daily soluble silver exposure dose is presented as a ratio between the measured silver concentration in blood (μg silver/kg blood) and the daily soluble silver (Ag ions) exposure dose (mg silver/kg body weight). The soluble silver exposure dose for Ag < 20 was calculated at 7% of the silver exposure dose (Ag ions and AgNPs) and at 100% for AgNO₃. (*) Significant difference of AgNPs vs AgNO₃ ($p < 0.05$).

glycerol trioleate/Tween 20 stabilized particles and PVP-coated particles, one study reported a higher release rate of silver ions from PVP-coated particles (50 ± 20 nm) in comparison to that from citrate capped AgNPs of the same size. Citrate has been suggested to act as a possible chemical barrier for silver ion dissolution.^{9,11} The results of the PVP-coated particles in the study by Kittler *et al.*, 2011¹¹ resemble our data and the stabilizing agents that are present in the Ag < 20 particle stock suspension (polyoxyethylene glycerol trioleate and Tween 20) might function as a coating through the same mechanism as citrate does, hereby effectively preventing ion dissolution. Consequently, the stable Ag < 20 particles were further regarded as model particles throughout the study to compare AgNP exposure with AgNO₃ exposure relative to the amount of soluble silver.

28-Day Oral Exposure Study. Rats were exposed daily for 28-days by oral gavage to 90 mg/kg body weight (bw) Ag < 20 or Ag < 15-PVP particles, to 9 mg/kg bw AgNO₃, or to their respective vehicle solutions only. The 10 times lower dose of AgNO₃ was intentionally chosen in the range of the soluble silver content in the Ag < 20 suspension. Two different negative control groups were included since the vehicle solution of the Ag < 20 particles contained additional AgNP stabilizing agents. At day 29 the animals were euthanized and organs were collected. Wash-out groups, identically exposed for 28-days to Ag < 20, Ag < 15-PVP, or AgNO₃, were euthanized at day 36 and 84.

Body and Organ Weights. All rats were weighed daily before, and weekly after day 36. The increase in body weight of the AgNP/AgNO₃ exposed rats was similar to that of the control groups, and also to the standard curve supplied by the breeder (data not shown). Also, organs from AgNP/AgNO₃ exposed rats, collected at day 29, 36, and 84, showed no significant differences in weight in comparison to the control groups (data not shown). Furthermore, no behavioral differences were

observed between the different groups throughout the study.

Silver Kinetics in Blood and Feces. Weekly, blood was drawn from the rats and feces was collected. In these samples the elemental silver content was determined. Since the exposure dose of silver was not equal in all groups (90 mg/kg bw for the Ag < 20 and Ag < 15-PVP groups vs 9 mg/kg bw for the AgNO₃ group), all results were normalized on the silver exposure dose and presented as the ratio between the measured silver concentration in blood or feces (μg silver/kg blood or feces) and the daily silver exposure dose (mg silver/kg body weight). Absolute measured silver concentrations in blood are given in the Supporting Information (Table S1). The blood and fecal silver contents in the control groups were below detectable levels ($<5 \mu\text{g}$ silver/kg blood and $<100 \mu\text{g}$ silver/kg feces), and are therefore not shown. Only a small difference in the blood silver content was detected between the animals treated with the Ag < 20 and Ag < 15-PVP particles (Figure 4A). However, the blood silver content in the AgNO₃ group was significantly higher than that of the AgNP groups at all time points during exposure. This clearly illustrates a much higher uptake of silver when AgNO₃ was administered compared to AgNPs. One day after the final exposure at day 28, a significant reduction in blood silver could already be detected in all groups and 1 week postexposure blood silver levels were reduced to a nondetectable level, indicating a rapid clearance of silver from the blood in all groups.

Figure 4A also shows that, during the first 28 days, the silver content in the blood of Ag < 20 and Ag < 15-PVP groups was approximately 7 to 10 times lower than that in the AgNO₃ group. From these findings we hypothesize that mainly the soluble silver, released from the nanoparticles, is bioavailable in the AgNP groups. To evaluate this hypothesis, the blood silver content was also normalized on the soluble silver exposure dose and presented as the ratio between

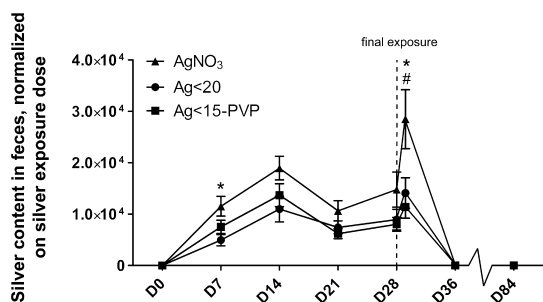


Figure 5. Silver content in feces (mean \pm SEM, $n = 5$) during 84 days. Results are normalized on the daily silver exposure dose and presented as a ratio between the measured silver concentration in feces (μg silver/kg feces) and the daily silver (Ag ions and AgNPs) exposure dose (mg silver/kg body weight). (*) Significant difference of AgNO₃ vs Ag < 15-PVP ($P < 0.05$); (#) significant difference of AgNO₃ vs Ag < 20 ($p < 0.05$).

the measured silver concentration in blood (μg silver/kg blood) and the daily soluble silver exposure dose (mg silver/kg body weight). The soluble silver exposure dose equals 7% of the silver exposure dose for Ag < 20, and 100% of the silver exposure dose for AgNO₃ (Figure 4B). We did not normalize the Ag < 15-PVP data, because the release of Ag⁺ from these particles is time-dependent (Table 2). Normalization on the soluble silver exposure dose indeed showed that the difference between Ag < 20 and AgNO₃ was much smaller compared to Figure 4A, although now, the plasma silver content in the Ag < 20 group was significantly higher than that in the AgNO₃ group. These data indicate that after oral exposure to AgNPs the major part of plasma Ag is ionic Ag released from the AgNPs. It may be argued though, that the AgNPs might dissociate to a higher extent *in vivo*, compared to *in vitro*, since a decrease in pH from 7.4 to 4.0 (like the stomach environment¹⁸) has been reported to increase the dissolution rate of silver ions from AgNPs.¹⁰ However, in a study performed in our laboratory using an *in vitro* digestion model, it was shown that the number, size, and the composition of AgNPs were not affected by the differences in pH (unpublished data). The soluble silver content, however, was not measured in this latter study.

Besides blood silver contents, also fecal silver contents were determined. Fecal sampling was performed by collecting a specimen weekly in the morning. Therefore, results on fecal silver content are merely indicative. After normalization on the silver dose that was used for exposure, the fecal silver content appeared to be similar between both AgNP groups during the entire study period (Figure 5). The silver content in the AgNO₃ group seemed a little higher than that in the AgNP groups, with significant differences on day 7 *versus* the Ag < 20 group, and on day 29 *versus* the Ag < 20 and Ag < 15-PVP group. After the final exposure at day 28, silver was rapidly eliminated

from the feces to a nondetectable level, 1-week post-exposure. The excreted Ag in the feces was estimated at about >99% of the intake, implying that only a minute fraction was absorbed. The low silver content of plasma is in agreement with this low absorption.

Distribution of Total Silver. To examine the distribution profile of silver in the different exposure groups, the total silver content was measured in a variety of organs that were collected at day 29. Results were again normalized on the silver exposure dose and are depicted in Figure 6A. Absolute measured silver tissue concentrations are given in the Supporting Information (Table S2). Silver concentrations in the blank control groups were below the limit of detection, and are therefore not shown. In all three groups, silver concentrations were highest in the emptied tissues of the gastrointestinal tract, although large differences between animals were observed, probably due to different passage times of the gastrointestinal contents. Next, the organs with the highest silver concentrations were the liver and spleen, followed by the testis, kidney, brain and lungs. Again, the uptake of silver was much higher in the AgNO₃ group in comparison to the AgNP groups, corroborating with the silver uptake results in blood. One striking observation was that there were no significant differences in distribution profiles between the two types of AgNPs. Apparently, the coating had no effect on the tissue distribution behavior.

After normalization of the silver contents in the organs on the soluble silver exposure dose, the AgNO₃ and Ag < 20 groups had similar silver contents in all organs except for the testis and spleen (Figure 6B), thereby further strengthening the hypothesis that mainly silver in a nonparticulate form is absorbed *via* the intestines. In a 28-day rat study, rats were orally exposed to PVP-coated AgNPs (14 nm) and silver acetate.⁸ The AgNP suspension contained 11% of soluble silver and results showed higher silver concentrations in several organs for the group receiving silver acetate (AgAc). This corroborates with our findings on the significantly higher absorption of silver in the soluble silver group *versus* the AgNP groups. In contrast to our work, these authors indicated that not only soluble silver, but also a significant fraction of AgNPs contributed to the silver in the organs of the AgNP group. In the present study, contribution of AgNPs to the silver concentration in organs was only observed in the testis and spleen and to a much lower extent. These inconsistencies might be explained by the use of different particles, or by the slight differences in exposure (twice a day *versus* the single exposure in our study). In fact, when considering the particles, even small variations in endless combinations of factors like size,¹⁹ surface charge, coatings, or stabilizers of the particles, or the concentration of the particles used for exposure^{4,12} can lead to a different distribution

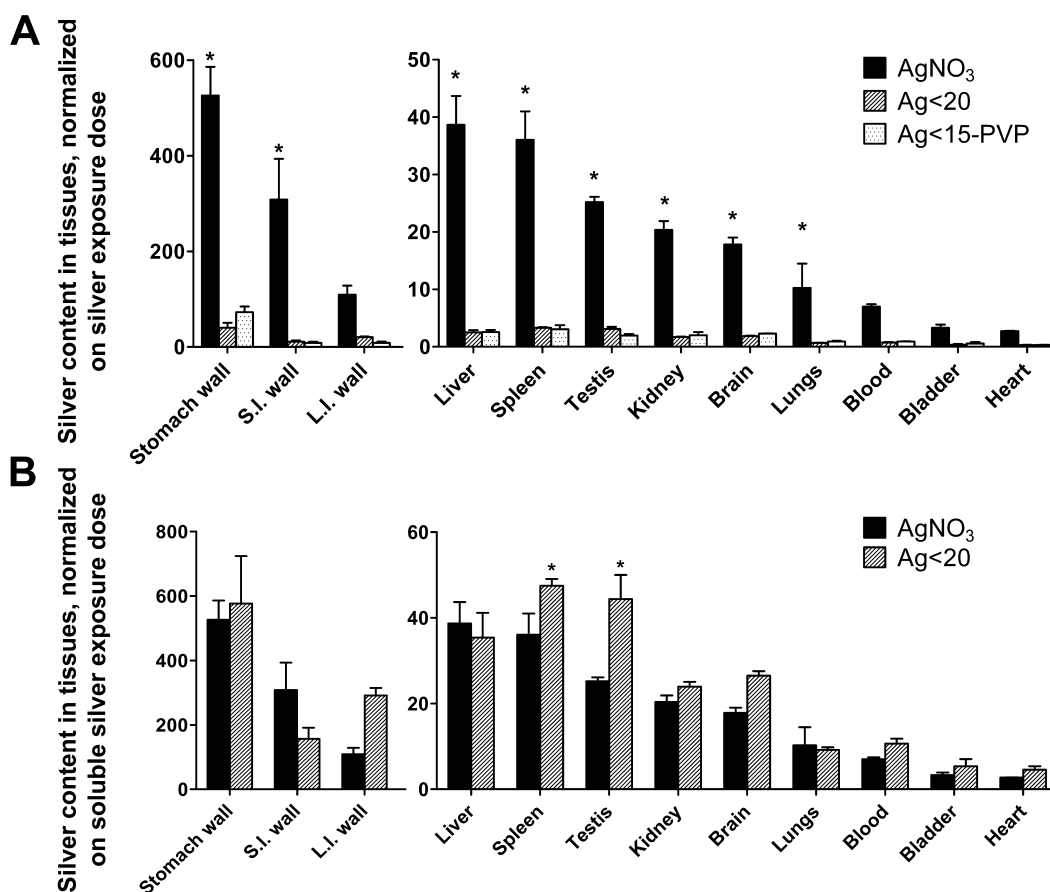


Figure 6. Silver content in tissues (mean \pm SEM, $n = 5$) at day 29. (A) The tissue silver content normalized on the daily silver exposure dose is presented as a ratio between the measured silver concentration in tissue (μg silver/kg tissue) and the daily silver (Ag ions and AgNPs) exposure dose (mg silver/kg body weight). (B) The tissue silver content normalized on the daily soluble silver exposure dose is presented as a ratio between the measured silver concentration in tissue (μg silver/kg tissue) and the daily soluble silver (Ag ions) exposure dose (mg silver/kg body weight). The soluble silver exposure dose for Ag < 20 was calculated at 7% of the silver exposure dose (Ag ions and AgNPs) and at 100% for AgNO₃. (*) Indicates statistically significant differences between the groups ($p < 0.05$). Abbreviations: S.I., small intestine; L.I., large intestine.

pattern. Subsequently, also the animal species, strain, age, breeding, and housing facilities, and inter-animal differences may have an impact on the outcome of the study. Clearly, more knowledge on the behavior of different types of AgNPs *in vivo* is required to fully understand and explain the distribution of AgNPs *in vivo*.

Previously, the liver and kidneys have been described as the primary organs for silver distribution, whether the exposure was orally,^{4,8,12,14} intravenously,^{19,20} subcutaneously,²¹ or through inhalation.²² Considering the biological clearance function of both the liver and kidneys, high silver concentrations in these organs may have been expected. In liver however, high silver concentrations may also be caused by accumulation of thiol-silver complexes, due to the high affinity of silver ions to sulfur containing groups that are commonly present in the liver.^{9,23} Deposition of silver in the liver has been detected in several cell types, including the K upffer cells, and the sinusoidal endothelium cells.^{12,24,25} In kidneys, deposition has been reported to occur in the renal glomerular basement membrane,^{24,26,27} and in the mesangium.²⁸

Besides the liver and kidneys, the spleen and testis also contained high amounts of silver. Two other oral exposure studies reported high distribution of silver to the testis as well,^{4,12} whereas high distribution to the spleen has been reported after intravenous exposure.¹⁹ However, the latter study showed a size-dependent distribution of AgNPs to the spleen, in which 80 and 110 nm particles resulted in high splenic distribution, while 20 nm particles did not.¹⁹

Silver was also distributed to the brain, which is in correspondence with previous reports as well.^{3,4,8,12,19,29–31} However, in most studies, including ours, it is not clear whether the silver is present in the brain endothelial cells or in the brain tissue. Therefore, it is not clear if the silver passed the blood-brain barrier. One study however, confirmed by TEM-energy dispersive X-ray spectrometry (EDX) the presence of AgNPs in neuronal cells after subcutaneous exposure.²¹ In comparison to other AgNP exposure studies,^{4,8,12,19} the silver content in the brain in our study appeared to be relatively high. The organs were not perfused before measurement in our study, so residual blood could have influenced the

TABLE 3. Retention of Silver in Several Organs at Day 36 and 84, Measured by AAS. Data Are Given As a Percentage \pm SEM of the Silver Concentrations Measured at Day 29 ($n = 5$)

	brain		testis		kidney		spleen	
	day 36	day 84	day 36	day 84	day 36	day 84	day 36	day 84
AgNO ₃	99 \pm 12%	100 \pm 5%	114 \pm 29%	94 \pm 11%	102 \pm 19%	60 \pm 16%	71 \pm 23%	22 \pm 7% ^a
Ag < 20	109 \pm 7%	95 \pm 7%	103 \pm 15%	76 \pm 11%	71 \pm 14%	27 \pm 3% ^a	52 \pm 8% ^a	13 \pm 1% ^a
Ag < 15-PVP	107 \pm 11%	94 \pm 5%	74 \pm 29%	34 \pm 13% ^{a,b}	37 \pm 11% ^{a,b}	0% ^{a,b}	21 \pm 2% ^a	7 \pm 2% ^a

^a Significant decrease in silver concentration versus day 29 ($p < 0.05$). ^b Significant decrease in silver concentration versus AgNO₃ at the same time point ($p < 0.05$).

measurements in organs with a high blood content, like the brain or lungs. Yet, the silver content in blood was 2–3 times lower than the silver content in brain, indicating that the contribution of silver in blood would probably be small. Evidence of silver transfer across the blood–brain-barrier is alarming, since neurotoxicity of silver in the brain has already been reported after systemic, intracerebral, and intranasal administration of AgNPs.^{32–35} The AgNPs were described to alter sensory, motor, and cognitive functions in mice, depending on the dose and duration of exposure.^{32–34} However, those studies did not include a soluble silver control to evaluate whether the effects were caused by the AgNPs or by the silver ions, but copper and aluminum nanoparticles were capable of inducing the same effects, suggesting that this was indeed related to the presence of metal-containing nanoparticles. Furthermore, intranasal exposure of AgNPs (30–380 nm) in rats at doses of 3 and 30 mg/kg bw has been described to induce brain edema, and damage to neurons, which resulted in learning and memory deficits, but also this study did not include a soluble silver control.³⁵

In the wash-out groups at days 36 and 84, the percentage of silver remaining in the organs was calculated on the basis of the results of day 29. In most tissues, silver concentrations were already significantly reduced below 50% one-week postexposure, and approached complete clearance in nearly all samples at day 84 (data not shown). However, four of the examined tissues behaved differently, namely brain, testis, kidney, and spleen (Table 3). Absolute measured silver concentrations in these tissues are given in the Supporting Information (Table S3). In brain and testis, 70 to 100% of the total silver at day 29 remained present 1-week postexposure (day 36) in all exposure groups. The silver levels in the brain were still above 90% even 2 months postexposure. In the testis the silver concentration was decreased slightly more after this time period, but was still above 70% for the AgNO₃ and Ag < 20 group, and above 30% in the Ag < 15-PVP group. In the kidney and spleen, more than 50% of the silver remained in the AgNO₃ and Ag < 20 groups after 1 week. After 2 months, the silver content dropped significantly, with the exception of the silver content in the kidney for the AgNO₃ group that was still above

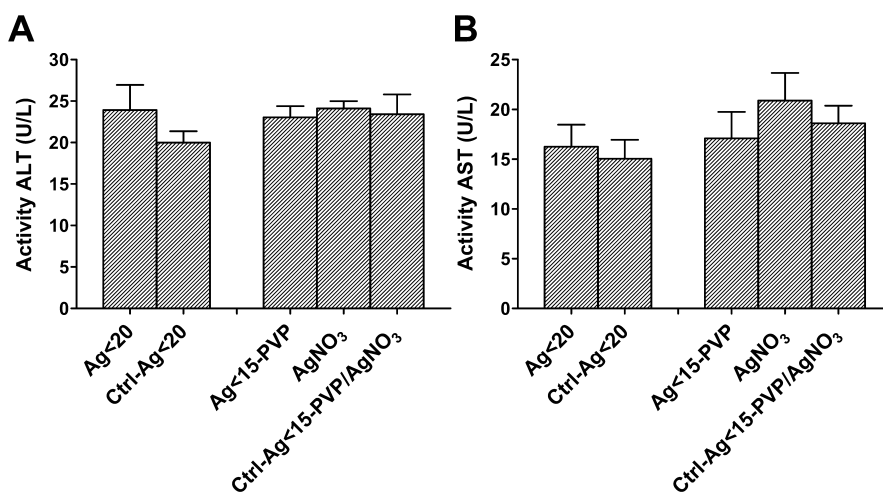
50%. Silver content in the kidney and spleen was already low 1-week postexposure for the Ag < 15-PVP group, and almost negligible after 2 months. In contrast to the distribution results at day 29, the two types of nanoparticles gave different results in time, although these differences were not significant at the various time points. The clearance of silver from the tissues of the rats that were exposed to the Ag < 15-PVP particles seemed to occur twice as fast as in the rats that were exposed to the Ag < 20 particles. This difference, however, might not be due to the difference between the particles, it could possibly be attributed to the absolute silver concentration in the tissues. The absolute silver concentrations in the tissues of the Ag < 15-PVP exposed rats were approximately two times lower at day 29 (Supporting Information: Table S3) than those in the tissues of the Ag < 20 exposed rats. Clearance from the tissues might be dose dependent, where lower concentrations are cleared quicker than higher concentrations.

The presence of silver in the brain is alarming, due to the potential risks mentioned previously, but the observation that silver remains present in the brain is even more disturbing. An older study from the 1980s showed that intraperitoneally injected silver distributed to the brain and remained present at least 13 months. The silver content started decreasing only after 4 to 8 months.²⁹ This suggests that accumulated silver in the brain can be expected to be long lasting.

Retention of silver has also been studied by others in liver, lung, and kidney, after a single intravenous dose of AgNPs (~8 nm). For three days, there was a rapid decline in silver content in liver and lung tissue, but not in the kidneys.²⁰ These results nicely correspond to the results of our study, where clearance from the kidney also appeared to progress more slowly. A single subcutaneous injection with AgNPs (50–100 nm) has been reported to induce prolonged accumulation of silver up to 24 weeks in the kidney, liver, spleen, brain, lung, and blood, which is significantly different from our results.²¹ It must be noted that the particles reached their maximum concentrations in the organs only after 12 to 24 weeks, probably due to the administration route. The particles that were used in that study were poorly characterized.

TABLE 4. Presence of Silver Containing Nanoparticles in Organs ($n = 5$), and Sizes of Detected Nanoparticles, Measured by SP-ICP-MS at Day 29

	# of animals positive for the presence of nanoparticles			average particle size (nm)		
	AgNO ₃	Ag < 20	Ag < 15-PVP-PVP	AgNO ₃	Ag < 20	Ag < 15-PVP-PVP
stomach content	3	1	1	26	32	32
S.I. content	4	3	2	23	24	28
L.I. content	5	4	5	23	29	30
liver	5	5	5	24	24	24
spleen	2	3	2	23	22	22
lungs	0	1	1	ND	20	26

**Figure 7. Enzyme activity levels in plasma (mean ± SEM, $n = 5$) at day 29 of (A) ALT and (B) AST.**

Currently, to our knowledge, no studies described the behavior of silver in testis. However, the finding of silver accumulating in testis is of high concern and extremely important to explore further.

Distribution of Silver Containing Nanoparticles. Measurements of the total silver content in organs does not provide information about whether the silver is present in soluble or particulate form. We therefore applied SP-ICP-MS to detect silver containing nanoparticles in several tissues taken at day 29, 36, and 84 and in the gastrointestinal contents. Results from day 29 indicated that both AgNP groups and the AgNO₃ group contained nanoparticles in the liver, spleen, and lungs, as well as in the gastrointestinal contents one day after the final exposure (Table 4). No nanoparticles were detected in the control groups nor in all groups at days 36 and 84.

Quite remarkable was the detection of silver containing nanoparticles in the AgNO₃ group, indicating that nanoparticles were formed *in vivo* from soluble silver. The exact composition of the particles cannot be determined with SP-ICP-MS, since the technique is limited to single element detection, due to the extremely short dwell times that are necessary for particle detection. Several possibilities can be envisaged for the *in vivo* formation of silver salts, like AgS, AgSe, or AgCl from soluble silver ions. This is very likely

to happen, especially considering the high binding affinity to sulfur, which is commonly present in cellular structures, and the high abundance of chloride *in vivo*.⁹ This theory is supported by the results of a study performed in our laboratory, in which AgNPs and AgNO₃ were immersed in gastrointestinal juices using an *in vitro* digestion model (unpublished data). Here, nano-sized silver salts containing sulfur and chloride were formed from AgNO₃ in the intestinal juices. The presence of silver salts has been described in the intestines in rats (AgS and AgSe) after oral exposure to AgAc,⁸ and in the kidneys of mice (AgS) after oral exposure to AgNO₃.²⁴ Furthermore, complex formation of AgS and AgSe was also reported to occur in the skin of argyria patients.³⁶ Formation of AgCl has been described in an *in vitro* study, in which PVP-coated AgNPs strongly reacted with HCl.³⁷ Since soluble silver is also present in the AgNP groups, there is a possibility that silver salts were formed in these groups as well.

It cannot be excluded that only a subpopulation of larger AgNPs was detected in the tissues. The sizes of the nanoparticles approached the minimum measurable size of the SP-ICP-MS technique, which is approximately 20 nm. Thus, AgNPs smaller than 20 nm are not detected. Also the AgNP concentrations in the measured tissues and gastrointestinal contents

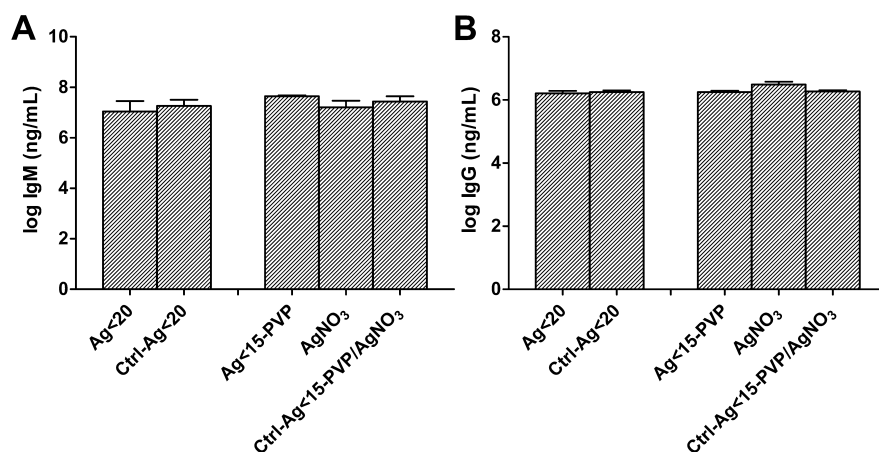


Figure 8. Antibody levels in plasma (mean \pm SEM, $n = 5$) at day 29 of (A) IgM and (B) IgG.

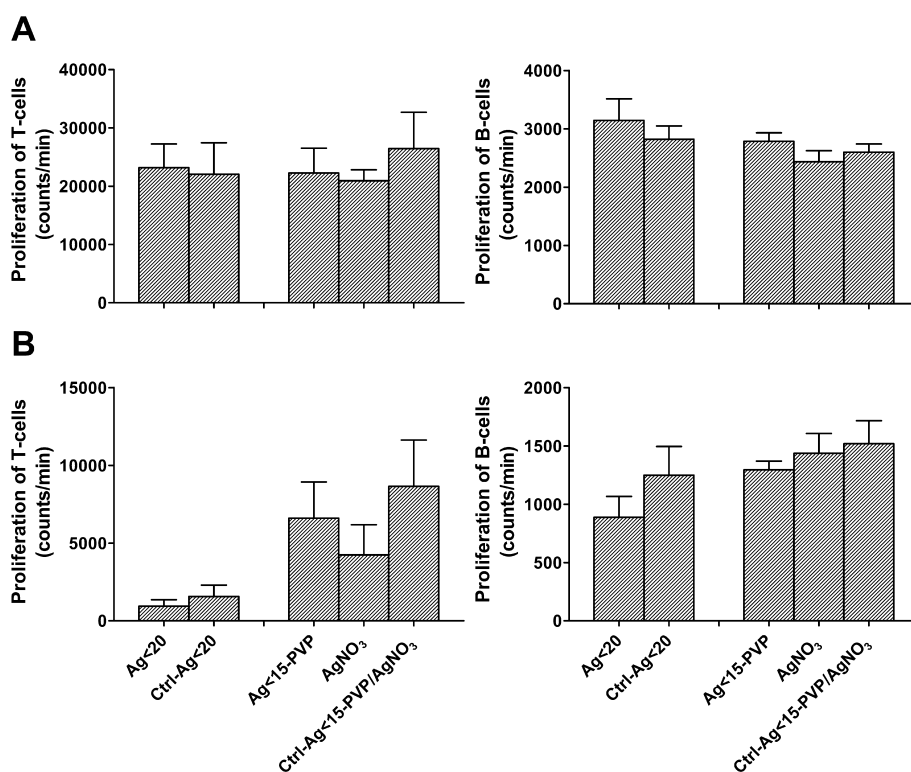


Figure 9. Proliferation of lymphocytes (mean \pm SEM, $n = 5$), isolated from the (A) Spleen and (B) MLN.

approached the detection limits of the SP-ICP–MS technique. So, our measurements are possibly an underestimation, which is why the exact concentration of AgNPs in the tissues could not be determined.

Blood Biochemical Analysis. Aberrant expression of AST and ALT in blood is indicative of injury to the liver. Results of the biochemical analysis of these two markers in plasma at day 29 are shown in Figure 7. Plasma levels of all silver exposed groups were compared to each other, as well as to their respective control groups. In all groups the absolute levels of AST and ALT in plasma were relatively low compared to reference values^{38,39} and no significant differences were detected in either comparison, signifying that there is

no indication of acute hepatotoxicity. However, even though AST and ALT markers in blood are not significantly increased, some mild adverse responses in liver might still occur. Our findings on the AST and ALT levels in the AgNP exposed groups are consistent with two previously reported 28-day AgNP oral exposure studies.^{4,12} In these studies, varying concentrations of AgNPs, of approximately 60 nm, were used at doses that far exceeded the dose used in the present study. No differences in AST or ALT levels were reported, but there were significant increases in cholesterol and alkaline phosphatase levels (also markers indicative for liver damage) for the higher dosage groups (>500 mg/kg bw) and histopathological analysis of the liver

TABLE 5. Cytokine Levels in pg/mL (Mean \pm SEM, $n = 5$) in Cell Culture Medium from LPS Stimulated Lymphocytes, Isolated from Spleen and MLN at Day 29

	Ag < 20	Ctrl-Ag < 20	Ag < 15-PVP	AgNO ₃	Ctrl-Ag < 15-PVP/AgNO ₃
Cells Isolated from Spleen; LPS Treated					
IL-1 β	4674 \pm 105	4104 \pm 158	4344 \pm 183	4156 \pm 169	4292 \pm 112
IL-6	11661 \pm 252	10248 \pm 610	10957 \pm 559	9747 \pm 286	10813 \pm 361
IL-10	27221 \pm 1090	23815 \pm 1131	24466 \pm 1164	23353 \pm 984	24715 \pm 121
TNF α	7886 \pm 52 ^a	6211 \pm 229	7311 \pm 200	6480 \pm 40	7248 \pm 203
Cells Isolated from MLN; LPS Treated					
IL-1 β	1688 \pm 84	1460 \pm 102	1889 \pm 55	1663 \pm 61	1758 \pm 164
IL-6	4507 \pm 656	5178 \pm 473	5535 \pm 478	5380 \pm 362	5396 \pm 581
IL-10	13488 \pm 873	14284 \pm 360	15029 \pm 404	15024 \pm 699	14871 \pm 1039
TNF α	1687 \pm 284	1663 \pm 190	2151 \pm 219	1774 \pm 150	2076 \pm 215

^a Significant variation versus the respective control group ($p < 0.05$).

TABLE 6. Cytokine Levels in pg/mL (mean \pm SEM, $n = 5$) in Cell Culture Medium from ConA Stimulated Lymphocytes, Isolated from Spleen and MLN at day 29

	Ag < 20	Ctrl-Ag < 20	Ag < 15-PVP	AgNO ₃	Ctrl-Ag < 15-PVP/AgNO ₃
Cells Isolated from Spleen; ConA Treated					
IL-1 β	198 \pm 14	316 \pm 61	192 \pm 22 ^a	207 \pm 9	383 \pm 63
IL-6	86 \pm 12	260 \pm 89	81 \pm 12 ^a	83 \pm 6 ^a	389 \pm 102
IL-10	4887 \pm 248	6208 \pm 1127	4246 \pm 415	5958 \pm 453	6591 \pm 722
TNF α	1574 \pm 168	1713 \pm 350	1662 \pm 157	1626 \pm 175	1711 \pm 112
INF γ	3213 \pm 152	2954 \pm 299	3060 \pm 65	3155 \pm 93	2817 \pm 298
IL-2	4189 \pm 366	5354 \pm 698	4555 \pm 341	4499 \pm 265	5459 \pm 302
IL-4	37 \pm 4	29 \pm 6	32 \pm 3	33 \pm 7	32 \pm 2
IL-13	9 \pm 2	16 \pm 5	7 \pm 0.3	10 \pm 2	27 \pm 9
IL-17 α	932 \pm 89	1023 \pm 167	689 \pm 54	1457 \pm 385	1525 \pm 250
Cells Isolated from MLN; ConA Treated					
IL-1 β	59 \pm 16	41 \pm 18	61 \pm 5	52 \pm 6	57 \pm 18
IL-6	59 \pm 32	29 \pm 6	79 \pm 28	72 \pm 9	161 \pm 37
IL-10	2190 \pm 132	2017 \pm 240	2511 \pm 59	2746 \pm 193	3003 \pm 369
TNF α	715 \pm 188	862 \pm 203	1193 \pm 154	1077 \pm 117	1057 \pm 109
INF γ	2146 \pm 534	2362 \pm 198	2911 \pm 432	2049 \pm 152	279 \pm 577
IL-2	1521 \pm 567	1536 \pm 388	2756 \pm 443	2657 \pm 331	2711 \pm 405
IL-4	20 \pm 4	17 \pm 3	24 \pm 2	19 \pm 2	32 \pm 4
IL-13	ND	ND	ND	ND	ND
IL-17 α	127 \pm 33	135 \pm 32	231 \pm 61	182 \pm 66	328 \pm 131

^a Significant variation versus the respective control group ($p < 0.05$).

showed dose-dependent exposure effects, including a slightly increased incidence of bile duct hyperplasia, with or without necrosis.^{4,12} Subchronic inhalation of AgNPs has also been described to result in similar histopathological findings in liver as described above without induction of AST or ALT levels in blood.^{3,40}

Immunotoxicity Analysis. Several approaches were applied to evaluate whether oral exposure to AgNPs induced immunotoxic responses. The determination of IgM and IgG levels in plasma indicated that exposure to silver did not affect total serum IgG and IgM levels (Figure 8). Additionally, proliferation of mitogenically stimulated T- or B-cells, isolated from the spleen and MLN, was not significantly altered in the exposure groups (Figure 9). Furthermore, cytokine levels in the supernatants of these stimulated T- and B-cells were

unaffected in the exposure groups (Tables 5 and 6). Finally, the activity of NK-cells, isolated from the spleen, was unaffected by the silver exposure (Figure 10). Taken together, these results indicate that oral AgNP exposure does not result in nonspecific immune responses *in vivo*. *In vitro* studies on the other hand, have proven the release of several cytokines to be increased by AgNP exposure to macrophages,^{41,42} and human peripheral blood mononuclear cells (PBMCs).⁴³ However, in our study the cytokine levels were measured to assess whether the responses of lymphocytes to the stimuli ConA and LPS were impaired by *in vivo* AgNP exposure, in contrast to assessing whether AgNPs affect the response *in vitro*. Nevertheless, the *in vitro* study with human PBMCs, reported that T-cell proliferation in response to ConA was not affected by AgNP

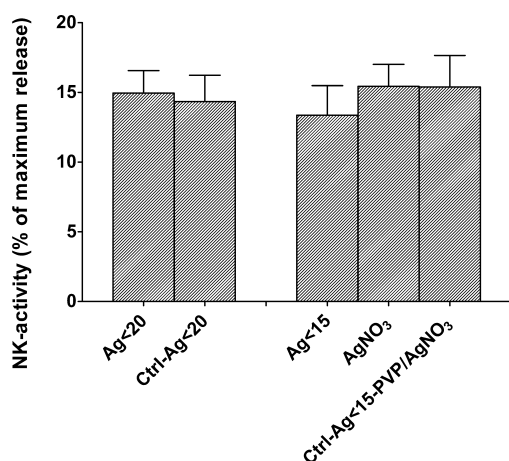


Figure 10. Activity of NK-cells (mean \pm SEM, $n = 5$), isolated from the spleen, as a percentage of the maximal release of radioactivity from ⁵¹Cr-labeled YAC-1 target cells.

exposure, which is in line with the results of the present study.⁴³

CONCLUSION

It can be concluded that the main target organs for silver distribution upon oral exposure of two AgNPs and AgNO₃ are the liver and spleen, followed by the testis, kidney, brain, and lungs, without differences in

the distribution pattern between the two different AgNPs, or the AgNO₃ exposed animals. The uptake of silver in blood and organs was higher in the AgNO₃ exposed rats than in the AgNP exposed rats. When taking only the fraction of soluble silver into account, the proportions of silver taken up of the Ag < 20 and AgNO₃ were rather similar. This indicates that silver is probably mainly bioavailable in the ionic form and not in the particulate form after AgNP exposure. However, not all measured silver could be accounted for in blood, testis, and spleen by the fraction of soluble silver alone, indicating that a small fraction of particles might be bioavailable as well. Elimination of silver occurred at an extremely slow rate in brain and testis, which still contained high concentrations of silver two months after the final exposure. Silver containing nanoparticles were detected with SP-ICP-MS in liver, spleen, and lungs of all AgNP exposed animals, but also of the AgNO₃ exposed animals. Clearly, nanoparticles are formed *in vivo* from silver ions and they are probably composed of silver salts.

When these results are taken together, it appears as if oral exposure to AgNPs is very similar to exposure to silver salts. However, the consequences of the *in vivo* formation of silver containing nanoparticles and of the long retention of silver in brain and testis should be considered in a risk assessment of AgNPs.

METHODS

Nanomaterials. An aqueous stock suspension of noncoated AgNPs (NM-300K; referred to as Ag < 20) with an average size < 20 nm and its matrix control (NM-300KDIS; referred to as Ctrl-Ag < 20) were obtained from the JRC repository (Ispra, Italy). The matrix consisted of the stabilizing agents polyoxyethylene glycerol trioleate (4%) and Tween 20 (4%) in H₂O. These particles are very well characterized by the manufacturer to allow their use as representative manufactured nanomaterials in the OECD testing program. This characterization consisted of TEM analysis, scanning electron microscopy (SEM) analysis and nanoparticle tracking analysis (NTA). Stock suspensions were diluted with liquid chromatography/mass spectrometry (LC/MS) grade water (Biosolve, Valkenswaard, The Netherlands) to a total silver concentration of 27 mg/mL. The matrix control was equally diluted.

Coated AgNPs (75 wt % PVP; Nanostructured & Amorphous Materials, Inc., Houston, USA, referred to as Ag < 15-PVP) with an average size < 15 nm, and AgNO₃ (Sigma-Aldrich, Zwijndrecht, The Netherlands) were obtained as dry powder. The Ag < 15-PVP particles were suspended in LC/MS grade water to a total silver concentration of 27 mg/mL and AgNO₃ was dissolved in LC/MS grade water to a final silver concentration of 2.7 mg/mL. Pure LC/MS grade water served as a matrix control for the Ag < 15-PVP particles and AgNO₃ (referred to as Ctrl-Ag < 15-PVP/AgNO₃). All suspensions/solutions were prepared freshly three times a week. To minimize agglomeration of the particles, the particle suspensions were sonicated for 20 min at 20 °C at 100% output (4 W specific ultrasound energy (240 J/m³)), using a Branson 5510 water bath sonicator (Emerson, USA) after preparation.

AgNP Suspension Characterization. The morphological characteristics of the AgNPs were analyzed by TEM. To reduce the risk of formation of possible artifacts, all TEM micrographs were analyzed on the same day the grids were prepared. The PVP

coating of the Ag < 15-PVP particles was analyzed only qualitatively by bringing a homemade pioloform- and carbon-coated EM-grid pretreated with 1% Alcian blue in contact with a droplet of a 1 mg/mL suspension of silver particles, as described by Mast and Demeestere 2009.⁴⁴ Grids were washed twice with double distilled water to remove excess particles. The grids were blotted using filter paper and subsequently stained with uranyl acetate, followed by examination with a Tecnai Spirit microscope (FEI, Eindhoven, The Netherlands) with an accelerating voltage of 120 kV. Digital micrographs were made using a bottom-mounted 4 × 4 K Eagle Camera. The negative staining allows visualization of the coating as a luminescent corona, while particles were detected on their inherent electron density.

The sizes of both types of AgNPs were analyzed qualitatively and quantitatively by bringing a homemade pioloform- and carbon-coated EM-grid pretreated with 1% Alcian blue in contact with a droplet of a 1 mg/mL suspension of silver particles and subsequently blotted using filter paper. Grids were washed twice with double distilled water to remove excess particles. Micrographs were taken using the same setup as described above. Magnification was set at 68000×, and about 10 points over the total grid were selected for systematic random sampling. Sizes of minimally 350 particles were semiautomatically quantified using Analysis Solution of the iTEM software (Olympus, Münster, Germany). A manual threshold was applied and particles were detected in a region of interest (ROI), excluding border particles and particles consisting of less than 50 or 100 pixels. For each particle the mean diameter was measured.

The hydrodynamic diameter of both types of AgNPs was analyzed by DLS analysis. Particle suspensions, at concentrations of 5 or 10 mg/L for the Ag < 20 and Ag < 15-PVP particles respectively, were prepared with ultrapure LC/MS water and sonicated at 100% output, using a Branson 5510 water bath sonicator for 20 min. DLS measurements were performed using an ALV dynamic light scattering setup (ALV-Laser

Vertriebsgesellschaft m-b.H., Hessen, Germany), consisting of a Thorn RFIB263KF photomultiplier detector, an ALV-SP/86 goniometer, an ALV 50/100/200/400/600 μm pinhole detection system, an ALV7002 external correlator, and a Cobolt Samba-300 DPSS laser, with a wavelength of 532 nm and a power of 300 mW. Each measurement consisted of 10 technical replicates and was conducted at a scattering angle of 90°. Hydrodynamic diameters were calculated using ALV software (AfterALV 1.0d, Dullware, USA).

Finally, the dissolution behavior of the AgNPs in suspension was analyzed in the Ag < 20 and Ag < 15-PVP suspensions. Silver ions, dissolved from AgNPs, highly attribute to the biological activity of AgNP suspensions and several factors might influence the dissolution of silver ions. Two factors of importance to the current study design, were examined, namely: different AgNP concentrations and varying storage times. AgNPs were extracted from the AgNP suspension to determine the ionic silver fraction. Ultrafiltration of the AgNPs was performed by centrifugation through a cellulose filter with a nominal cutoff value of 3 kDa (Ultra-4, Amicon). The total silver content in the unfiltered AgNP suspensions and their respective filtrates were measured by AAS. The percentage of soluble silver in the AgNP suspensions was calculated by dividing the silver content in the filtrates by the silver content in the unfiltered AgNP suspensions multiplied by 100. Ultrafiltration separation efficiency was verified by DLS (ALV setup and method as previously described) and ultraviolet–visible spectroscopy (UV–vis; UV-mini 1240; Shimadzu, Japan) analysis of the filtrates. The UV–vis spectroscopy analysis was performed by adding a volume of 1 mL to a quartz cuvette and measuring the absorption at a wavelength spectrum, ranging from 200 to 600 nm at room temperature. Binding of silver ions to the ultrafiltration membrane was also evaluated by preparing an AgNO₃ dilution series, ranging from 0.05 to 10 μg silver/mL, and processing them by ultrafiltration. The total silver content in the solution before and after filtration was measured by AAS. The influence of the silver concentration on the AgNP dissolution behavior was evaluated by preparing AgNP dilution series ranging from 5 to 100 μg silver/mL from nanoparticle stock suspensions of 27 mg silver/mL. Series were prepared in duplicate. The suspensions were immediately processed by ultrafiltration, followed by AAS measurement. The influence of time on the dissolution behavior of the particles was evaluated by ultrafiltration of particle suspensions (Ag < 20 with a concentration of 25 μg silver/mL and Ag < 15-PVP with a concentration of 12.5 μg silver/mL) at $T = 0, 1, 3, 6, 24, 48$ h and 7 days ($n = 2$), followed by AAS measurement.

In Vivo Experimental Design. Six-week-old male specific pathogen free Sprague–Dawley rats were purchased from Harlan (Horst, The Netherlands). At the start of the experiment the average body weight of the animals was ~ 245 g. Animals were housed in polycarbonate cages (maximum three per cage) with a 12 h light/dark reversed cycle and were allowed to acclimatize for two weeks before the start of the experiment. Room temperature was ~ 20 °C with a relative humidity of $\sim 55\%$. Food and water was given *ad libitum*, except for a two hour fasting period before each oral gavage. The study was performed according to the national guidelines for the care and use of laboratory animals under approval of the Dutch animal welfare committee.

Rats were randomly divided into 5 groups ($n = 5$ per group): (1) Ag < 20; 90 mg/kg bw (2) Ag < 15-PVP; 90 mg/kg bw, (3) AgNO₃ 9 mg/kg bw, (4) Ctrl-Ag < 20, and (5) Ctrl-Ag < 15-PVP/AgNO₃. In addition, the remaining rats were randomly divided into 3 groups ($n = 5$) to study the wash-out until day 36, and into another 3 groups ($n = 5$) to study the wash-out until day 84. These wash-out groups for day 36 and 84 received equal treatments as group 1–3.

All rats were exposed daily for 28 days by oral gavage. Dosing volume was 3.3 mL/kg bw. The suspensions/solutions were directly administered into the lower esophagus, only after 2 h of fasting, to prevent a reflux reaction. During the first 28 days, all animals were weighed daily. Weekly, 250 μL of blood was drawn on heparin through the tail vein, 5 h after the oral gavage. Blood was placed on ice for total silver measurements. Additionally, weekly, a sample of the feces was collected from

each rat just before the oral gavage for total silver measurements. At day 29, the first five groups were euthanized by CO₂/O₂ inhalation and the following organs were excised aseptically, weighed, and placed on ice: liver, kidneys, lungs, heart, spleen, brain, bladder, testis, and the MLNs. Furthermore, blood was collected on heparin and stored on ice, as well as the stomach and small and large intestinal wall, and their carefully separated contents. Whole blood was used for total silver measurements and heparinized plasma was extracted from the remaining blood by centrifugation of the blood for 15 min at 3000g and collection of the upper layer.

After day 29, the animals in the wash-out groups were weighed daily and feces was collected weekly. At day 36, three wash-out groups for day 36 were randomly euthanized by CO₂/O₂ inhalation and organs were collected, weighed, and stored according to the same protocol as applied on day 29.

The remaining three wash-out groups for day 84 were weighed weekly from day 37 to day 84, and feces was collected weekly. Blood (250 μL) was drawn on heparin through the tail vein every other week and placed on ice until silver measurements. At day 84, all animals were euthanized, and the organs were collected according to the same protocol as applied on day 29.

Determination of total Silver Content in Suspensions, Tissues, Organs and Gastrointestinal Content. Total silver content was determined in the AgNP/AgNO₃ stock suspensions/solutions, and in the AgNP/AgNO₃ dilution series with their respective filtrates, as obtained from the AgNP dissolution characterization. Before AAS measurement, AgNP suspensions and AgNO₃ solutions were digested by weighing ~ 1 g suspension and adding it to 10 mL of a mixture of concentrated hydrochloric- and sulphuric acid (3:1), followed by a microwave treatment of 90 min at ~ 250 °C, 70 bar. The acidic mixture to digest silver suspensions is different to that used to digest tissue samples, since the presence of an excess of chloride (which is commonly present in tissue samples) was found to be imperative for complete dissolution of the silver nanoparticles.⁹ Tissue samples of day 29, 36, and 84 (liver, kidneys, lungs, heart, spleen, brain, bladder, testis, and the stomach-, large- and small intestinal wall) as well as whole blood samples were digested by weighing ~ 1 g tissue or blood in 10 mL of nitric acid 70%, followed by a microwave treatment of 90 min at ~ 250 °C, 70 bar. Whole blood instead of plasma was used for total silver measurements to avoid loss of silver during the separation process. Blood that was collected through the tail vein during the first 28 days was pooled per group to obtain enough material for measurement. Upon cooling, the digests were further diluted by adding purified water to a total volume of 50 mL. Subsequently, samples were measured on a AAnalyst 800 (Perkin-Elmer, USA). The resulting silver concentrations were expressed in $\mu\text{g}/\text{kg}$, with a limit of detection of 5 $\mu\text{g}/\text{kg}$ for blood and 100 $\mu\text{g}/\text{kg}$ for all organs, gastrointestinal contents, and feces. The results of the silver measurements were corrected for an overall recovery of 70%. The recovery was determined by measuring AgNO₃ and AgNP dilution series in LC/MS grade water, and by measuring liver and kidney tissue spiked with AgNO₃ or AgNPs. Digested tissues were spiked at concentrations ranging from 0.05 to 100 mg/L. Silver dilution series ranged from 5 to 100 $\mu\text{g}/\text{mL}$.

Determination of AgNPs in Tissues and Gastrointestinal Content. Samples of stomach and small and large intestinal content, liver, spleen, kidney, and lungs from day 29, 36, and 84 were prepared for SP-ICP–MS analysis by enzymatic digestion. In short, 2 mL of digestion buffer (10 mM Tris, 1% Triton X-100, and 1 mM calcium acetate; pH 9.5; Sigma Aldrich) was added to 200 mg of tissue. The suspension was vortexed for 15 s. Subsequently, 625 μL of proteinase K (32 U/mL; Sigma-Aldrich) was added, mixed by 10 s vortexing, and incubated for 16 h at 55 °C in a shaking water bath. After incubation the mixture was vortexed vigorously for 1 min and further diluted 40000 times with purified water. Blood samples were immediately diluted 40000 times with purified water. Samples were analyzed on a Thermo X Series 2 (Waltham, MA, USA), equipped with an auto-sampler, a Babington nebulizer, and operated at a radio frequency (RF) power of 1400 W. Silver was measured at m/z (molecular mass/number of elementary charges) values of 107 and 109.

Data acquisition was performed using Thermo Plasmalab software in the time-resolved analysis (TRA) mode with a dwell time of 3 ms and an acquisition time of 60 s per measurement. Data were exported as a CSV file and processed in Microsoft Excel. Particle sizes, size distributions, and concentrations were calculated. Results were corrected for blank samples. The particle sizes are calculated from the measured silver masses by assuming a spherical shape of the particles. The lower size detection limit of SP-ICP-MS for AgNPs is ~ 20 nm, while the concentration detection limits depended on the quantity of the available samples and on the preparation procedure. The concentration detection limits were set at 40 $\mu\text{g/L}$ for blood, 400 $\mu\text{g/kg}$ for all organs, and 2 mg/kg for the gastrointestinal contents (which equals $\sim 2 \times 10^{12}$ particles/L blood, $\sim 2 \times 10^{13}$ particles/kg organ, and $\sim 8 \times 10^{13}$ particles/kg gastrointestinal content, respectively, assuming a particle size of ~ 20 nm).

Blood Biochemical Analysis. In blood plasma, taken at day 29, ALT and AST activity was analyzed using an AST and ALT kit based on the LiqulUV modified International Federation of Clinical Chemistry and Laboratory Medicine (IFCC) method (INStruChemie, Delfzijl, The Netherlands). Measurements were performed according to the instructions in the kit. A volume of 200 μL of heparinized plasma was pipetted into a cuvette and placed in a water bath at 25 $^{\circ}\text{C}$. Following, 1 mL of enzyme reagent (25 $^{\circ}\text{C}$) was added to the cuvette and incubated for 5 min at 25 $^{\circ}\text{C}$. After exactly 5 min, 250 μL of substrate reagent was added and mixed. The absorbance was read after exactly 1, 2, 3, and 4 min at 340 nm. Enzyme activity (U/L) was calculated by multiplying the average change in absorbance per minute with 952.

Immunotoxicity Analysis. Cell Isolation. Excised MLNs and approximately one-third of the spleen of each rat were stored separately in Iscove's modified Dulbecco's medium (IMDM; Gibco, Grand Island, NY, USA) on ice. The organs were pressed gently through a cell strainer (70 μm nylon; Falcon, Becton-Dickinson Labware, Franklin Lakes, NJ, USA) and the cells were suspended in 25 mL of IMDM, supplemented with 10% fetal calf serum (FCS; PAA, Linz, Austria), 100 IU/mL penicillin, and 100 $\mu\text{g/mL}$ streptomycin, referred to as complete Iscove's medium. The cell suspensions were centrifuged at 300g for 10 min (4 $^{\circ}\text{C}$), and the pellets were resuspended in 20 mL of complete Iscove's medium. Finally, cells were counted using a Coulter counter (Coulter Electronics, Luton, UK).

Lymphocyte Transformation Test. A total of 1.05×10^6 cells, isolated from the spleen or MLNs, was cultured in 6-fold in 150 μL of complete Iscove's medium in U-bottom 96-well microtiter plates (Greiner, Frickenhausen, Germany). To three of the six wells 0.3 μg of LPS or Con A was added. Plates were incubated for 48 h with LPS, or for 72 h with Con A in a humidified atmosphere containing 5% CO_2 at 37 $^{\circ}\text{C}$. Following, 37 kBq [methyl- ^3H]thymidine ([^3H]TdR; Amersham, Little Chalfont, UK) was added to the wells, and the cells were incubated for another 24 h. Finally, cells were harvested onto glass-fiber filters (LKB-Wallac, Espoo, Finland) using a multiple cell culture harvester (LKB-Wallac), and radioactivity was counted using a LKB Wallac 1205 Betaplate Beta Liquid Scintillation Counter (LKB-Wallac).

NK Activity Assay. Adherent cells were removed from spleen cell suspensions by overnight incubation at 37 $^{\circ}\text{C}$ as described elsewhere.⁴⁵ The activity of NK cells was measured by the ability of 2×10^6 spleen cells to lyse 1×10^4 ^{51}Cr -labeled yeast artificial chromosome-1 (YAC-1) target cells during a 4 h coinubation in 96-well cell culture plates (Greiner) at 37 $^{\circ}\text{C}$. Radioactivity was then counted using a Perkin-Elmer Packard Cobrall Auto Gamma Counter. NK-cell activity was given as a percentage of the maximal release by YAC cells, calculated as (radioactivity counts in the supernatant minus the spontaneous release by YAC)/(maximal release by YAC cells minus the spontaneous release by YAC cells).

Cytokine Release. MLN and spleen cells were incubated with LPS and Con A using the same cell concentrations and LPS and Con A concentrations as described above.

A 4-plex panel (IL-1 β , IL-6, IL-10, and TNF- α ; Bio-Rad, Hercules, CA, USA) was used for supernatants of LPS stimulated cells, while a 9-plex panel (IFN- γ , IL-1 β , IL-2, IL-4, IL-6, IL-10, IL-13, IL-17A, and TNF- α ; Bio-Rad) was used for supernatants of Con A stimulated cells. Analysis was performed according to the

instructions in the kit. Briefly, a volume of 100 μL of Bio-Plex assay buffer (Bio-Rad) was added to 96-wells filter bottom plates (Bio-Rad) to prewet the plate, and throughout the assay buffer was removed by vacuum after each incubation or wash step. Beads were diluted in assay buffer, and 50 μL /well was added. Then, the plates were washed 2 times with 100 μL of Bio-Plex wash buffer (Bio-Rad). Dilution series of the cytokine standards were made ranging from 32000 to 0.18 pg/mL. Fifty microliters of the standards and cell culture supernatants was added to the wells, and the plates were vortexed at 1100 rpm for 30 s and incubated at room temperature (RT) for 30 min while vortexing at 300 rpm. After incubation, the plates were washed three times with 100 μL of wash buffer. Detection antibody was diluted in detection antibody diluent (Bio-Rad), and 25 μL /well was added. The plates were again vortexed at 1100 rpm for 30 s, incubated at RT for 30 min while vortexing at 300 rpm and washed three times with 100 μL assay buffer. Next, streptavidin-phycoerythrin was diluted in assay buffer and 50 μL /well was added. The plates were incubated for 10 min at RT. After three times washing with 100 μL of wash buffer the beads were resuspended in 125 μL assay buffer and read on a Bio-Plex reader (Bio-Rad). Results were obtained at low photomultiplier tube settings.

Plasma IgG and IgM Levels. Plasma IgG and IgM levels were measured in plasma using rat IgG and IgM ELISA kits (E25G and E25M, respectively; ICL, Gentaur, The Netherlands). IgG was measured at 20 000-, 40 000-, and 80 000-fold plasma dilutions, while IgM was measured at a 600-fold plasma dilution.

Statistical Analysis. Results of the AgNP size characterization by TEM analysis were statistically analyzed using SigmaPlot software (Systat Software Inc., Chicago, USA). Other results were statistically analyzed using Prism software (v5; GraphPad Software, Inc., La Jolla, USA). Body- and organ weights, lymphocyte transformation, NK-activity, and antibody- and cytokine release results were analyzed by a one-way ANOVA with a Bonferroni post-test. AAS and biochemical analysis results were analyzed by a two-way ANOVA with a Bonferroni post-test. A p -value of ≤ 0.05 was considered significant. Outliers in the AAS and cytokine release results were removed according to Chauvenet's criterion.

Conflict of Interest: The authors declare no competing financial interest.

Acknowledgment. The authors would like to thank S. van Oostrum, A. van Polanen, J. Verbunt from RIKILT, P. Beekhof, A. de Klerk, and H. Verharen from the RIVM, and R. Folkink from the Wageningen University and Research Centre for their excellent technical assistance. This research was commissioned and financed by the Dutch Ministry of Economic Affairs, Agriculture and Innovation.

Supporting Information Available: Additional details of results are included. This material is available free of charge via the Internet at <http://pubs.acs.org>.

REFERENCES AND NOTES

- Morones, J. R.; Elechiguerra, J. L.; Camacho, A.; Holt, K.; Kouri, J. B.; Ramirez, J. T.; Yacaman, M. J. The Bactericidal Effect of Silver Nanoparticles. *Nanotechnology* **2005**, *16*, 2346–2353.
- Maynard, A. D., Nanotechnology: A Research Strategy For Addressing Risk. *Project on Emerging Nanotechnologies*; Woodrow Wilson International Center for Scholars: Washington, DC, 2006; pp 1–41.
- Ji, J. H.; Jung, J. H.; Kim, S. S.; Yoon, J. U.; Park, J. D.; Choi, B. S.; Chung, Y. H.; Kwon, I. H.; Jeong, J.; Han, B. S.; *et al.* Twenty-Eight-Day Inhalation Toxicity Study of Silver Nanoparticles in Sprague-Dawley Rats. *Inhalation Toxicol.* **2007**, *19*, 857–871.
- Kim, Y. S.; Kim, J. S.; Cho, H. S.; Rha, D. S.; Kim, J. M.; Park, J. D.; Choi, B. S.; Lim, R.; Chang, H. K.; Chung, Y. H.; *et al.* Twenty-Eight-Day Oral Toxicity, Genotoxicity, and Gender-Related Tissue Distribution of Silver Nanoparticles in Sprague-Dawley Rats. *Inhalation Toxicol.* **2008**, *20*, 575–583.
- Jeong, G. N.; Jo, U. B.; Ryu, H. Y.; Kim, Y. S.; Song, K. S.; Yu, I. J. Histochemical Study of Intestinal Mucins after Administration of Silver Nanoparticles in Sprague-Dawley Rats. *Arch. Toxicol.* **2010**, *84*, 63–69.

6. Florence, A. T. Nanoparticle Uptake by the Oral Route: Fulfilling Its Potential? *Technologies* **2005**, *2*, 6.
7. Bouwmeester, H.; Poortman, J.; Peters, R. J.; Wijma, E.; Kramer, E.; Makama, S.; Puspitaningandita, K.; Marvin, H. J. P.; Peijnenburg, A. A. C. M.; Hendriksen, P. J. M. Characterization of Translocation of Silver Nanoparticles and Effects on Whole-Genome Gene Expression Using an *in Vitro* Intestinal Epithelium Coculture Model. *ACS Nano* **2011**, *5*, 4091–4103.
8. Loeschner, K.; Hadrup, N.; Qvortrup, K.; Larsen, A.; Gao, X.; Vogel, U.; Mortensen, A.; Lam, H. R.; Larsen, E. H. Distribution of Silver in Rats Following 28 Days of Repeated Oral Exposure to Silver Nanoparticles or Silver Acetate. *Part. Fibre Toxicol.* **2011**, *8*, 18.
9. Liu, J.; Sonshine, D. A.; Shervani, S.; Hurt, R. H. Controlled Release of Biologically Active Silver from Nanosilver Surfaces. *ACS Nano* **2010**, *4*, 6903–6913.
10. Liu, J.; Hurt, R. H. Ion Release Kinetics and Particle Persistence in Aqueous Nano-silver Colloids. *Environ. Sci. Technol.* **2010**, *44*, 2169–2175.
11. Kittler, S.; Greulich, C.; Diendorf, J.; Koller, M.; Eppler, M. Toxicity of Silver Nanoparticles Increases During Storage because of Slow Dissolution under Release of Silver Ions. *Chem. Mater.* **2010**, *22*, 4548–4554.
12. Kim, Y. S.; Song, M. Y.; Park, J. D.; Song, K. S.; Ryu, H. R.; Chung, Y. H.; Chang, H. K.; Lee, J. H.; Oh, K. H.; Kelman, B. J.; et al. Subchronic Oral Toxicity of Silver Nanoparticles. *Part. Fibre Toxicol.* **2010**, *7*, 20.
13. De Jong, W. H.; Hagens, W. I.; Krystek, P.; Burger, M. C.; Sips, A. J.; Geertsma, R. E. Particle Size-Dependent Organ Distribution of Gold Nanoparticles after Intravenous Administration. *Biomaterials* **2008**, *29*, 1912–1919.
14. Park, E. J.; Bae, E.; Yi, J.; Kim, Y.; Choi, K.; Lee, S. H.; Yoon, J.; Lee, B. C.; Park, K. Repeated-Dose Toxicity and Inflammatory Responses in Mice by Oral Administration of Silver Nanoparticles. *Environ. Toxicol. Pharmacol.* **2010**, *30*, 162–168.
15. Klein, C. L.; Comero, S.; Stahlmecke, B.; Romazanov, J.; Kuhlbusch, T. A. J.; Van Doren, E.; De Temmerman, P.-J.; Mast, J.; Wick, P.; Krug, H. et al., NM-Series of Representative Manufactured Nanomaterials; NM-300 Silver Characterisation, Stability, Homogeneity. Joint Research Center: Luxembourg, 2011; pp 1–84.
16. Ahamed, M.; Posgai, R.; Gorey, T. J.; Nielsen, M.; Hussain, S. M.; Rowe, J. J. Silver Nanoparticles Induced Heat Shock Protein 70, Oxidative Stress and Apoptosis in *Drosophila Melanogaster*. *Toxicol. Appl. Pharmacol.* **2010**, *242*, 263–269.
17. Cumberland, S. A.; Lead, J. R. Particle Size Distributions of Silver Nanoparticles at Environmentally Relevant Conditions. *J. Chromatogr., A* **2009**, *1216*, 9099–9105.
18. McConnell, E. L.; Basit, A. W.; Murdan, S. Measurements of Rat and Mouse Gastrointestinal pH, Fluid and Lymphoid Tissue, and Implications for *in-Vivo* Experiments. *J. Pharm. Pharmacol.* **2008**, *60*, 63–70.
19. Lankveld, D. P.; Oomen, A. G.; Krystek, P.; Neigh, A.; Troost-de Jong, A.; Noorlander, C. W.; Van Eijkeren, J. C.; Geertsma, R. E.; De Jong, W. H. The Kinetics of the Tissue Distribution of Silver Nanoparticles of Different Sizes. *Biomaterials* **2010**, *31*, 8350–8361.
20. Park, K.; Park, E. J.; Chun, I. K.; Choi, K.; Lee, S. H.; Yoon, J.; Lee, B. C. Bioavailability and Toxicokinetics of Citrate-Coated Silver Nanoparticles in Rats. *Arch. Pharmacol. Res.* **2011**, *34*, 153–158.
21. Tang, J.; Xiong, L.; Wang, S.; Wang, J.; Liu, L.; Li, J.; Yuan, F.; Xi, T. Distribution, Translocation and Accumulation of Silver Nanoparticles in Rats. *J. Nanosci. Nanotechnol.* **2009**, *9*, 4924–4932.
22. Takenaka, S.; Karg, E.; Roth, C.; Schulz, H.; Ziesenis, A.; Heinzmann, U.; Schramel, P.; Heyder, J. Pulmonary and Systemic Distribution of Inhaled Ultrafine Silver Particles in Rats. *Environ. Health Perspect.* **2001**, *109*, 547–551.
23. Tiwari, D. K.; Jin, T.; Behari, J. Dose-Dependent *in-Vivo* Toxicity Assessment of Silver Nanoparticle in Wistar Rats. *Toxicol. Mech. Methods* **2011**, *21*, 13–24.
24. Danscher, G. Light and Electron Microscopic Localization of Silver in Biological Tissue. *Histochemistry* **1981**, *71*, 177–186.
25. Furchner, J. E.; Richmond, C. R.; Drake, G. A. Comparative Metabolism of Radionuclides in Mammals-IV. Retention of Silver-110m in the Mouse, Rat, Monkey, and Dog. *Health Phys.* **1968**, *15*, 505–514.
26. Ham, K. N.; Tange, J. D. Silver Deposition in Rat Glomerular Basement Membrane. *Aust. J. Exp. Biol. Med. Sci.* **1972**, *50*, 423–434.
27. Moffat, D. B.; Creasey, M. The Distribution of Ingested Silver in the Kidney of the Rat and of the Rabbit. *Acta Anat. (Basel)* **1972**, *83*, 346–355.
28. Day, W. A.; Hunt, J. S.; McGiven, A. R. Silver Deposition in Mouse Glomeruli. *Pathology* **1976**, *8*, 201–204.
29. Rungby, J.; Danscher, G. Localization of Exogenous Silver in Brain and Spinal Cord of Silver Exposed Rats. *Acta Neuropathol.* **1983**, *60*, 92–98.
30. Garza-Ocanas, L.; Ferrer, D. A.; Burt, J.; Diaz-Torres, L. A.; Cabrera, M. R.; Rodriguez, V. T.; Rangel, R. L.; Romanovicz, D.; Jose-Yacaman, M. Biodistribution and Long-Term Fate of Silver Nanoparticles Functionalized with Bovine Serum Albumin in Rats. *Metalomics* **2010**, *2*, 204–210.
31. Genter, M. B.; Newman, N. C.; Shertzer, H. G.; Ali, S. F.; Bolon, B., Distribution and Systemic Effects of Intranasally Administered 25 nm Silver Nanoparticles in Adult Mice. *Toxicol. Pathol.* **2012**.
32. Sharma, H. S.; Ali, S. F.; Hussain, S. M.; Schlager, J. J.; Sharma, A. Influence of Engineered Nanoparticles from Metals on the Blood-Brain Barrier Permeability, Cerebral Blood Flow, Brain Edema and Neurotoxicity. An Experimental Study in the Rat and Mice Using Biochemical and Morphological Approaches. *J. Nanosci. Nanotechnol.* **2009**, *9*, 5055–5072.
33. Sharma, H. S.; Hussain, S.; Schlager, J.; Ali, S. F.; Sharma, A. Influence of Nanoparticles on Blood-Brain Barrier Permeability and Brain Edema Formation in Rats. *Acta Neurochir. Suppl.* **2010**, *106*, 359–364.
34. Sharma, H. S.; Sharma, A. Neurotoxicity of Engineered Nanoparticles from Metals. *CNS Neurol. Disord. Drug Targets* **2012**, *11*, 65–80.
35. Liu, Y.; Guan, W.; Ren, G.; Yang, Z. The Possible Mechanism of Silver Nanoparticle Impact on Hippocampal Synaptic Plasticity and Spatial Cognition in Rats. *Toxicol. Lett.* **2012**, *209*, 227–231.
36. Massi, D., S. M. Human Generalized Argyria: A Submicroscopic and X-ray Spectroscopic Study. *Ultrastruct. Pathol.* **1998**, *22*, 47–53.
37. Li, L.; Zhu, Y. J. High Chemical Reactivity of Silver Nanoparticles toward Hydrochloric Acid. *J. Colloid Interface Sci.* **2006**, *303*, 415–418.
38. Aleman, C. L.; Mas, R. M.; Rodeiro, I.; Noa, M.; Hernandez, C.; Menendez, R.; Gamez, R. Reference Database of the Main Physiological Parameters in Sprague-Dawley Rats from 6 to 32 Months. *Lab. Anim.* **1998**, *32*, 457–466.
39. Petterino, C.; Argentino-Storino, A. Clinical Chemistry and Haematology Historical Data in Control Sprague-Dawley Rats from Pre-clinical Toxicity Studies. *Exp. Toxicol. Pathol.* **2006**, *57*, 213–219.
40. Sung, J. H.; Ji, J. H.; Park, J. D.; Yoon, J. U.; Kim, D. S.; Jeon, K. S.; Song, M. Y.; Jeong, J.; Han, B. S.; Han, J. H.; et al. Subchronic Inhalation Toxicity of Silver Nanoparticles. *Toxicol. Sci.* **2009**, *108*, 452–461.
41. Martinez-Gutierrez, F.; Thi, E. P.; Silverman, J. M.; de Oliveira, C. C.; Svensson, S. L.; Hoek, A. V.; Sanchez, E. M.; Reiner, N. E.; Gaynor, E. C.; Prydzial, E. L.; et al. Antibacterial Activity, Inflammatory Response, Coagulation and Cytotoxicity Effects of Silver Nanoparticles. *Nanomedicine (Philadelphia, PA, U.S.)* **2012**, *8*, 328–336.
42. Park, J.; Lim, D. H.; Lim, H. J.; Kwon, T.; Choi, J. S.; Jeong, S.; Choi, I. H.; Cheon, J. Size Dependent Macrophage Responses and Toxicological Effects of Ag Nanoparticles. *Chem. Commun. (Cambridge, U.K.)* **2011**, *47*, 4382–4384.
43. Greulich, C.; Diendorf, J.; Gessmann, J.; Simon, T.; Habijan, T.; Eggeler, G.; Schildhauer, T. A.; Eppler, M.; Koller, M. Cell Type-Specific Responses of Peripheral Blood Mononuclear Cells to Silver Nanoparticles. *Acta Biomater.* **2011**, *7*, 3505–3514.

44. Mast, J.; Demeestere, L., Electron Tomography of Negatively Stained Complex Viruses: Application in Their Diagnosis. *Diagn. Pathol.* **2009**, *4*.
45. de Jong, W. H.; Steerenberg, P. A.; Ursem, P. S.; Osterhaus, A. D.; Vos, J. G.; Ruitenber, E. J. The Athymic Nude Rat. III. Natural Cell-Mediated Cytotoxicity. *Clin. Immunol. Immunopathol.* **1980**, *17*, 163–172.